Structure of Octacyanocopperphthalocyanine Film Prepared by Chemical Vapor Deposition

Yasukiyo UEDA* and Michio ASHIDA*

Thin films were prepared on the substrate by the reaction of *1, 2, 4, 5*-tetracyanobenzene with copper film at various temperatures. The films were characterized by IR and UV/VIS spectroscopies. The fine strucure of the films was observed by high-resolution electron microscopy. The films produced on copper film below 400°C and above 450°C consisted of octacyanocopperphthalocyanine ($CuPc(CN)_8$) and poly-CuPc, respectively. The film produced above 450°C was composed of amorphous and continuous layer of poly-CuPc. On the other hand, the film produced below 400°C was composed of tentacle-like crystallites of $CuPc(CN)_8$. The molecular image of the crystal indicates that the crystal is a $CuPc(CN)_8$-Cu complex. The crystal structure of the complex is determined from electron micrographs. The unit-cell dimensions are $a=b=1.63$ nm, $c=0.68$ nm and the space group is P4/mcc. The molecular arrangement in the crystal was determined directly from the molecular images.

KEY WORDS: Thin organic film/ Characterization/ Phthalocyanine/ Crystal structure/ Chemical vapor deposition/

INTRODUCTION

In recent years, attempts have been made to prepare many organic compounds in the form of an ultrathin film and study the relation between the physical properties and molecular arrangements in the films. The techniques for preparing organic thin films can be divided into two types of processes: dry and wet. The Langumuir-Blodgett (L-B) method has been well developed as a wet process, and the properties of L-B films have been reported by many workers[1]. In the case of chemical vapor deposition (CVD) method as a dry process, there have been many reports on the structure and physical properties of inorganic compounds[2-5], but few reports on those of organic compounds[6-8]. In a previous paper[9], thin film of *2, 3, 9, 10, 16, 17, 23, 24*-octacyanodipotassiumphthalocyanine ($K_2Pc(CN)_8$) was prepared directly on substrate by the CVD reaction of *1, 2, 4, 5*-tetracyanobenzene (TCNB) with KCl crystal. The crystal structure determined from high-resolution electron micrograph suggested that the film was composed of $K_2Pc(CN)_8$-K complex crystallites. The similar crystallites were observed in the film prepared by the CVD reaction of TCNB with copper film[10].

The present study is concerned with the characterization of the films prepared by the CVD reaction of TCNB with copper film used as the substrate. The characterization of the films was investigated by IR and UV/VIS spectroscopies and the fine structure of the films was observed by electron microscopy.

---

* 上田裕清, 芦田道夫 : Faculty of Engineering, Kobe University, Rokkodai, Nada-ku, Kobe 657.

EXPERIMENTAL

A sample of TCNB was synthesized by two step procedure starting from pyromellitic dianhydride by the method of Bailey et al[11]. The crude TCNB was purified by recrystallization from acetic acid. A copper film vacuum-evaporated on KCl was used as a substrate. The refined TCNB powder of about 10 mg and the substrate was sealed in an evacuated pyrex glass tube at about 80 Pa after flushing with argon gas. The tube was heated at a temperature from 300 to 500°C for 10 hours in a hot air oven. The produced films were milled and pressed together with the KCl substrates and their IR spectra were examined by a JASCO A-302 IR spectrometer by the tablet method. The films were dissolved in concentrated surfuric acid and their UV/VIS spectra were obtained by a Shimazu UV-240 spectrometer. The film was separated from substrate in water, and the residual copper film was dissolved away in dilute nitric acid solution. The specimen film was mounted on a micro grid coated with an evaporated gold film. The high-resolution electron micrographs were obtained with a minimum exposure device. The electron microscopes were operated at 200 kV with microscope parameter of spherical aberration constants of either 2.0 mm or 1.4 mm. The (111) lattice images from the gold ($d=0.235$ nm) provided an accurate magnification calibration. The unit cell dimensions were accurately determined from electron diffraction patterns, using the lattice spacings of gold as reference. Image simulations were performed by a multislice program developed on an NEC PC-9801VM micro-computer equipped with a PC-9801-22 arithmetic operation co-processor and 640 KB RAMs[12].

RESULTS AND DISCUSSION

Green colored films were formed on the substrate by reaction of TCNB at temperatures of between 300 and 400°C and a gray film with metallic gloss was formed on the substrate above 450°C. The former films were soluble in concentrated sulfuric acid but the latter film had a very limited solubility. Figure 1 shows the UV/VIS absorption spectra of sulfuric acid solutions of the films produced at various temperatures. The films produced at the temperature between 300 and 400°C showed the identical absorption bands as that of CuPc(CN)₈ reported by Wöhrle and Hündorf[13]. The spectra showed the maximum peak at 738 nm and shoulders at 691, 664, 640, 390 and 342 nm. The absorption hands in the 600-750 and 200-400 nm regions are assigned, respectively, as the Q-band and the Soret band caused by $\pi \to \pi^*$ transitions in phthalocyanine macrocycles. The absorption bands of the film produced above 450°C became broader and the maximum peak in the Q-band shifted to shorter wavelength by 10 nm than that of the film produced below 400°C. The blue shift of the Q-band have been observed for associated phthalocyanines[14], dimeric phthalocyanines[15] and cofacially polymerized phthalocyanines[16], and has been discussed in terms of exciton coupling[17], which is based on the interaction between the excited states of Pc molecules. Therefore, it is considered that the soluble portion of the film produced above 450°C is associated or oligomeric CuPc(CN)₈ and that the insoluble portion of the film is polymerization
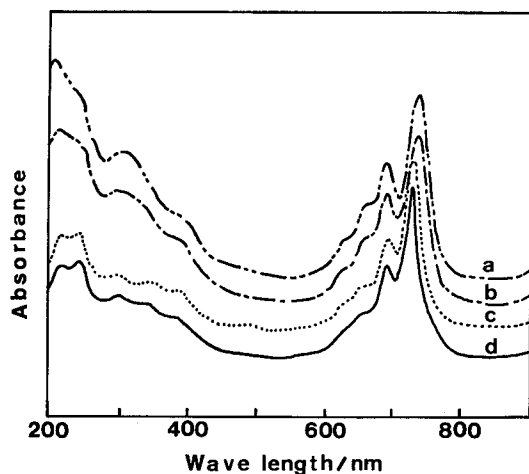
Fig. 1. UV/VIS spectra (in concd sulfuric acid) of films produced on copper film at 300°C (a), 350°C (b), 400° C (c) and 450°C (d).
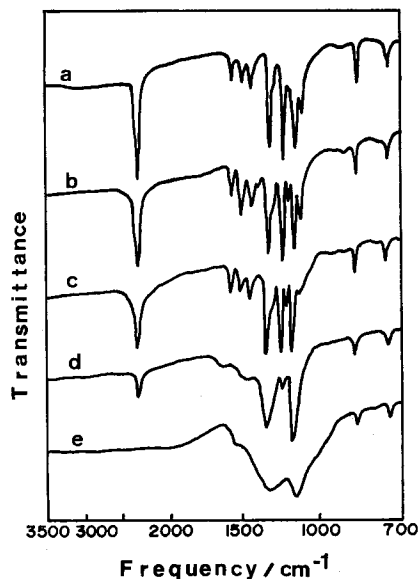
Fig. 2. IR spectra of films produced on copper film at 300°C (a), 350°C (b), 400°C (c), 450°C (d) and 500°C (e).

products.   Figure 2 shows the IR absorption spectra of the films produced on the substrate at various reaction temperatures.   The spectra of the films at the temperature from 300 to 400°C show the same absorption bands.   These spectra was similar to that of $CuPc(CN)_8$[13].   The absorption bands in a range from 1,000 to 1,600 cm^{-1} are characteristic ones of phthalocyanines, which are assigned to C-C and C-N stretching in Pc skeleton.   The absorption band with high intensity at 2,230 cm^{-1} are ascribed to a C≡N stretching of peripheral nitril groups of $CuPc(CN)_8$ molecule.   The spectrum of the film produced at 450°C showed some sign of the structural change.   The nitrile absorption at 2,230 cm^{-1} decreased to a small band and other absorption bands were broader than the respective ones of the films produced below 400°C.   The spectrum of the film produced at 500°C showed a broad band without fine structure between 1,600 and 1,000 cm^{-1} and no nitrile band at 2,230 cm^{-1}.   The ratio of absorption intensities, log (I_{2230}/I_{1095}), reveals the quantitative value of the nitrile groups per phthalocyanine unit[18].   These ratios were 0.88, 0.78, and 0.55 for the films produced at 300, 350 and 400°C, respectively.   It suggests that the nitrile groups per phthalocyanine unit decrease gradually in the films with elevating of reaction temperature.   Consequently, it seems that Pc units polymerized by peripheral nitrile groups to form poly-CuPc.   The poly-CuPc is considered to correspond to the insoluble portion of the film in concentrated surfuric acid.   On the basis of these results, it is concluded that the products formed below 400°C are identified as $CuPc(CN)_8$ and ones formed above 450°C as poly-CuPc.

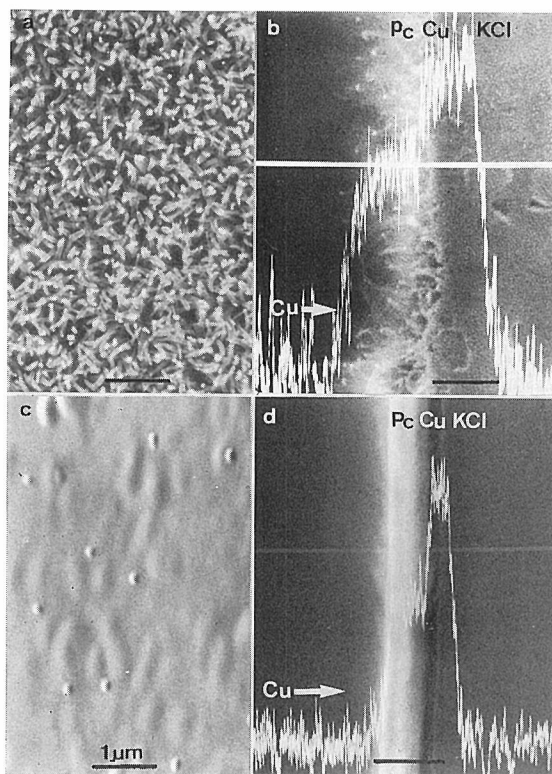The films produced on the substrate were observed by scanning electron

Fig. 3. Scanning electron micrographs of the surface and X-ray microanalyses of the cross section of CuPc(CN)$_8$ (a), (b) and poly-CuPc (c), (d) films.

microscopy, as shown in Fig. 3. The CuPc(CN)$_8$ film produced below 400°C are composed of twisted needle-like crystals standing on the substrate surface as is shown in Fig. 3(a). The poly-CuPc film produced above 450°C is composed of amorphous layer with roughly flat face as is shown in Fig. 3(c). The distribution of copper in the cross sections of the films is shown in Figs. 3(b), (d). The electron beam was scanned from surface to bottom of the film along the line as shown in the figure. Distribution of copper in both films showed to be uniform from bottom to surface. This finding indicates that the copper atom diffuses uniformly in the films.

The fine structure of needle-like CuPc(CN)$_8$ crystal was investigated by high-resolution electron microscope. In the first step of the CVD reaction, the CuPc(CN)$_8$ film was composed of discrete disk-like or lamellar crystallites as shown in Fig. 4(a). The electron diffraction pattern from the disk-like crystallite represents the single net pattern with D$_{4h}$, corresponding to the interplanar spacing of 1.63 nm, as shown in Fig. 4(b). The high-resolution electron micrograph from the disk-like crystallite showed a grid pattern with the spacing of 1.63 nm as shown in Fig. 5(a). The optical diffraction pattern from the electron micrograph shows D$_{4h}$ symmetry composed of square lattice points of 1.63 nm spacing as shown in
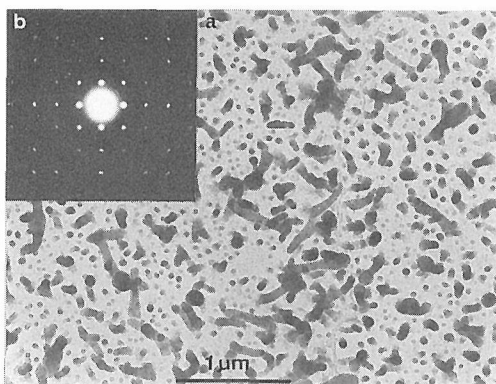
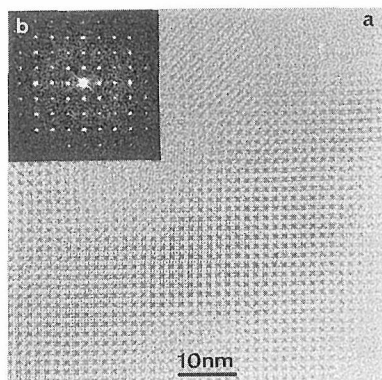Fig. 4. Transmission electron micrograph (a) and electron diffracton pattern (b) of $CuPc(CN)_8$ film.

Fig. 5. Electron micrograph (a) of the disk-like crystallites in $CuPc(CN)_8$ film and optical diffraction pattern (b) from a crystallite.

Fig. 5(b). This pattern is in good agreement with the corresponding electron diffraction pattern. The optical transform confirms that the real image of Fig. 5(a) was recorded at about 50 nm under focus in consideration of the scattering band from the carbon film superimposed on the crystalline pattern. The enlarged and noise-reduced high-resolution electron micrographs are shown in Fig. 6 together with reproduction of $H_2Pc(CN)_8$-K crystal[9]. From the analogy between two images, it is suggested that $CuPc(CN)_8$ crystal is isomorph of $H_2Pc(CN)_8$-K crystal. As reported previously[9], the planar molecules of $H_2Pc(CN)_8$ were in a layer normal to the c-axis and were located at the corners of the square lattice. $H_2Pc(CN)_8$ molecules staggered alternately from the a-axis by 27.4° to form the complex between peripheral nitrile groups and intercalated potassium atom. By comparison with a molecular image of $H_2Pc(CN)_8$-K, the rings of about 0.6 nm in diameter on the corners of the square in Fig. 6(a) are attributed to $CuPc(CN)_8$ molecules stacked parallel on a substrate. It is noteworthy that a high-contrast dot is observed in Pc ring of $CuPc(CN)_8$ molecules. The Pc ring of $K_2Pc(CN)_8$ molecules appeared to be open circle, because $K_2Pc(CN)_8$ molecule is easily demetalized to a metal free
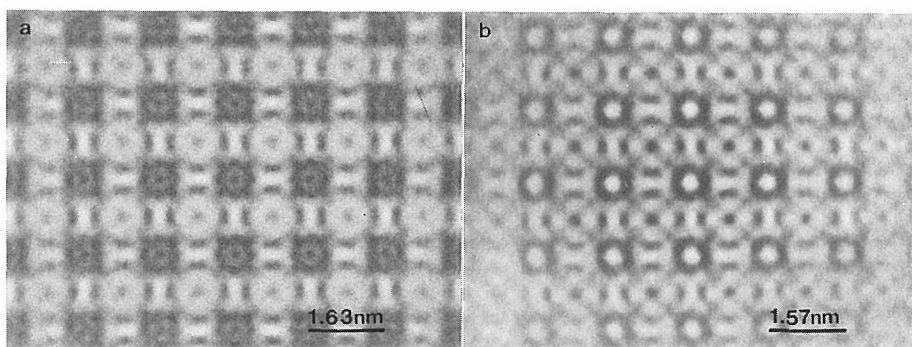

Fig. 6. High-resolution structure images of $CuPc(CN)_8$-Cu (a) and $H_2Pc(CN)_8$-K (b) complex crystals.

derivative (H$_2$Pc(CN)$_8$) in water[19]. On the other hand, MPc's such as CuPc, FePc and NiPc are not demetalized even in acid solutions. Therefore, the high-contrast dot in Pc ring is attributed to the copper atom. A high-contrast dot appears in the center of the square lattice. Similar dot was observed in the molecular image of H$_2$Pc(CN)$_8$-K complex crystal and was attributed to potassium atom. According to the elemental analysis[20], the films produced on the substrate at 350°C was found to be Cu$_{2.5}$C$_{40}$N$_{16}$H$_9$ (C, 55.1; H, 1.06; N, 25.6; Cu, 18.2%). Comparison of the C/Cu ratio of the product with that of CuPc(CN)$_8$ reveals that copper atom is included in the product more than that required for coordination in phthalocyanine ring. It is well-known that an organic molecule containing the nitrile group such as tetracyanoquinodimethane (TCNQ) forms the charge transfer complex with metal atom such as Al, Ag and Cu[21,22]. Therefore, it seems that a high-contrast dot at the center of the square is attributed to copper atom. A high-resolution micrograph of lamellar crystallites showed lattice fringes with 1.63 nm spacing as shown in Fig. 7. Parallel stripes with 0.34 nm interval are observed normally to the fringes.
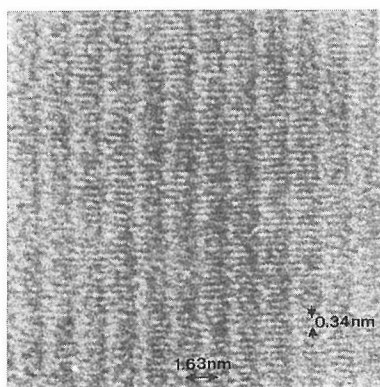

Fig. 7. Electron micrograph of a lamellar crystal in CuPc(CN)$_8$ film.

Each stripe corresponds to the image of the CuPc(CN)$_8$ molecule viewed along the molecular plane. Comparing the molecular and column images of CuPc(CN)$_8$-Cu complex crystal of those of H$_2$Pc(CN)$_8$-K complex crystal, a molecular arrangement of CuPc(CN)$_8$-Cu crystal was assumed to be similar to that of H$_2$Pc(CN)$_8$-K crystal, as shown in Fig. 8. Each CuPc(CN)$_8$ molecule (a) locates at the corners of a square with the lattice constant a of the tetragonal unit cell. Planar molecules are in a layar being perpendicular to the column axis (c-axis) and stagger by a rotation angle $\pm\omega$ to the a-axis alternately in successive layers, as shown in Figs. 8(b) and (c). These molecules are piled up with a interplanar distance of 0.34 nm along the c-axis, and copper atom is intercalated at the center of the square between two layers. The crystal projected along the c-axis gives a superposition of atoms as shown in Fig. 8(d). In the CuPc(CN)$_8$-Cu crystal, the intercalated copper is surrounded by a distorted cube of eight peripheral nitrile groups from each molecule situated at the corner of the two layers. Other nitrile groups are
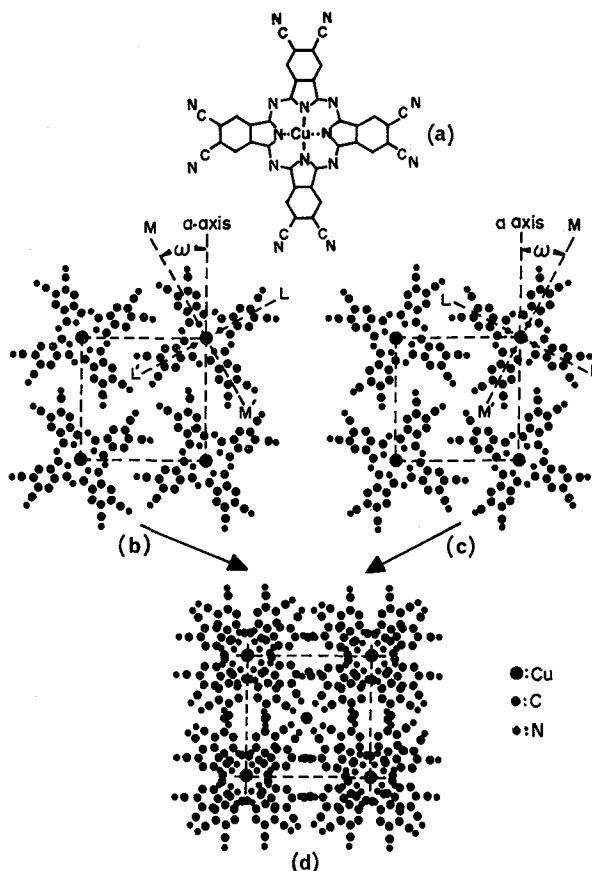
Fig. 8. Molecular structure of CuPc(CN)₈ (a) and molecular
arrangements projected along the *c*-axis: (b), (c) mole-
cules in two succesive layers; (d) schematic diagram
of the crystal structure projected along the *c*-axis.

overlapped almost parallel between the adjacent columns to countervalance opposite polarities of nitrile groups. Considering such molecular arrangements in the crystal, the unit-cell dimensions of CuPc(CN)$_8$-Cu crystal are $a=b=1.63$ nm, $c=0.68$ nm, and the space group is P4/mcc.

It is assumed that during the CVD reaction of TCNB with copper film cyclotetramerization of TCNB occurs on copper and subsequently TCNB reacts with copper diffusing through the substrate. Thus, the producting CuPc(CN)$_8$ molecules crystallized in the form of CuPc(CN)$_8$-Cu complex crystal by the inter-action between pheripheral nitrile groups and copper atom in the similar way to H$_2$Pc(CN)$_8$-K crystal. However, the cell parameter a of CuPc(CN)$_8$-Cu crystal is slightly longer than that of H$_2$Pc(CN)$_8$-K crystal. This difference of the distance between adjacent columns may be caused by the interaction and the size of inter-calated metals. The effect of intercalated metals induces slight change of the rotation angle of Pc molecules in the complex crystals. The rotation angle ω is determined by comparison the real image to computer simulated images. Calcu-
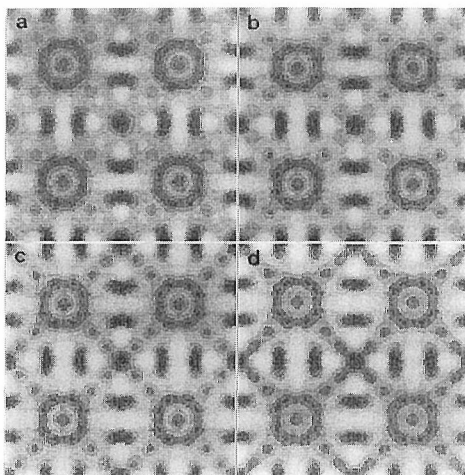
Fig. 9. Simulated images in the projection along the c-axis at various rotation angles: (a) 26°, (b) 27°, (c) 28°, (d) 29°.

lations were carried out for Cs=1.4 mm at 200 kV accelerating, Δf=50 nm under focus and the crystal thickness of 4.08 nm which corresponds to the value, about 4 nm, obtained by the mesh-holding method[12] of the film. Figure 9 shows the simulated images calculated by taking account of various rotation angle ω. These images reveal that the contrast distribution is very sensitive to the change of ω. The crossed rod at the center of each image becomes clear in contrast with increasing rotation angle, and those at the angles of 28° and 29° show a higher density than that of the real image. Furthermore, the parallel bars linking the Pc rings become shorter with increasing rotation angle. In order to determine the rotation angle more quantitatively, the attention is given to two values of n and
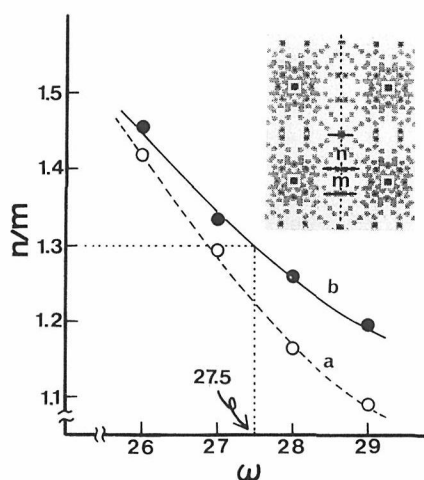

Fig. 10. Plots of the n/m ratio obtained from potential maps (a) and the simulated images (b) against the rotation angle.

m which are the distance between the dot located at the center and the short bar linked $CuPc(CN)_8$ rings and one between parallel bars, respectively, as superimposed in Fig. 10. The n/m ratio is plotted against various angles ω. The n/m ratio obtained from potential map, which represents the atomic position in the crystal, decreases with the increase of ω. It is well-known that image contrast in the electron micrograph is affected significantly by the value of defocus and crystal thickness, as well as the operating condition of electron microscope. Consequently, the n/m ratio obtained from the simulated image taking the microscopic parameters into consideration was used to determine the rotation angle. The n/m ratio from the simulated image is bigger than that from the potential at the same rotation angle. The observed value from the real image shown in Fig. 6(a) was 1.3. Therefore, the rotation angle ω in $CuPc(CN)_8$-Cu crystal was determined to be 27.5°, which is coincided to that of $H_2Pc(CN)_8$-K crystal[9,12]. This finding seems to suggest that the lattice constant a of the complex crystal depends on the interaction between peripheral nitrile groups of $MPc(CN)_8$ and intercalated atom. The interaction based on the electron configuration of intercalated atom will be described in detail elsewhere.

ACKNOWLEDGEMENTS

REFERENCES

(1) *Thin Solid Films*, 132–134 (1983).
(2) A.S. Jordan, A.V. von Neida, R. Caruso and C.K. Kim, *J. Electrochem. Soc.*, **121**, 153 (1974).
(3) G.R. Srinivasan, *J. Electrochem. Soc.*, **127**, 1334 (1980).
(4) B.V. Spitsyn, L.L. Bouilov and B.V. Derjauin, *J. Cryst. Growth*, **52**, 219 (1981).
(5) P.M. Razeghi, B. de Cremoux and J.P. Duchemin, *J. Cryst. Growth*, **68**, 389 (1984).
(6) W.F. Gorham, *J. Polym. Sci. A-1*, **4**, 3027 (1966).
(7) A.A. Berlin and A.I. Sherle, *Inorg. Macromol. Rev.*, **1**, 253 (1971).
(8) M. Tsuji, S. Isoda, M. Ohara, A. Kawaguchi and K. Katayama, *Polymer*, **23**, 1568 (1982).
(9) M. Ashida, Y. Ueda, H. Yanagi, N. Uyeda, Y. Fujiyoshi and J.R. Fryer, *Acta Cryst.* **B44**, 146 (1988).
(10) Y. Ueda, M. Ashida, Y. Fujiyoshi, N. Uyeda and J.R. Fryer, *Proc. 11th Int. Congr. Electron Mirosc., Kyoto*, **vol. 2**, p. 1405 (1986).
(11) A.S. Bailey, R.B. Henn and J.M. Langdon, *Tetrahedron*, **19**, 161 (1963).
(12) H. Yanagi, S. Maeda, Y. Ueda and M. Ashida, *Ultramicroscopy*, **25**, 1 (1988).
(13) D. Wöhrle and U. Hündorf, *Makromol. Chem.*, **186**, 2177 (1985).
(14) A.T. Davidson, *J. Chem. Phys.*, **77**, 168 (1982).
(15) W.A. Nevin, M.R. Hempstead, W. Lin, C.C. Leznoff and A.B.P. Lever, *Inorg. Chem.*, **26**, 570 (1987).
(16) C.W. Dirk, T. Inabe, K.F. Schoch, Jr. and T.J. Marks, *J. Am. Chem. Soc.*, **105**, 1539 (1983).
(17) M. Gouterman, D. Holten and E. Lieberman, *Chem. Phys.*, **25**, 139 (1977).
(18) D. Wöhrle, U. Marose and R. Knoop, *Makromol. Chem.*, **186**, 2209 (1985).

(19) P.A. Barrett, C.E. Dent and R.P. Linstead, *J. Chem. Soc.*, 1719 (1936).
(20) M. Ashida, Y. Ueda, H. Yanagi and K. Sayo, *J. Polym. Sci. Polym. Chem. Ed.*, in press.
(21) N. Uyeda, T. Kobayashi and E. Suito, *Microscopic Electronique* 1970 **vol. 1** (ed. P. Favard) 443–444 (*Societe Francaise de Microscopic Electronique, Paris,* 1970).
(22) N. Uyeda, T. Kobayashi, K. Ishizuka and Y. Fujiyoshi, *Nature* **285**, 95 (1980).